IEEE Access
Multidisciplinary | Rapid Review | Open Access Journal

Received December 12, 2020, accepted December 31, 2020, date of publication January 6, 2021, date of current version January 13, 2021.

Digital Object Identifier 10.1109/ACCESS.2021.3049558

A Partial Discharge Localization Method in Transformers Based on Linear Conversion and Density Peak Clustering

SHUDONG WANG[1,3], (Graduate Student Member, IEEE), YIGANG HE[1,2], (Member, IEEE), BAIQIANG YIN[1], WENBO ZENG[1], YING DENG[1], AND ZENGCHAO HU[1]

[1]School of Electrical Engineering and Automation, Hefei University of Technology, Hefei 230009, China
[2]School of Electrical Engineering and Automation, Wuhan University, Wuhan 430072, China
[3]State Grid Anhui Electric Power Company Ltd., Electric Power Research Institute, Hefei 230031, China

Corresponding authors: Baiqiang Yin (yinbaiqiang123@163.com) and Yigang He (18655136887@163.com)

This work was supported in part by the National Natural Science Foundation of China under Grant 51977153, Grant 51977161, Grant 51577046, and Grant 61971175; in part by the State Key Program of National Natural Science Foundation of China under Grant 51637004; in part by the National Key Research and Development Plan "Important Scientific Instruments and Equipment Development" under Grant 2016YFF0102200; in part by the Equipment Research Project in Advance under Grant 41402040301; and in part by the Fundamental Research Funds for the Central Universities under Grant JZ2019YYPY0025.

ABSTRACT The detection of partial discharge (PD) is a crucial method to evaluate the insulation status of transformers. The main difficulties of the current localization algorithms are the complexity of the solution and sensitivity to time delay errors. This article proposes a PD localization method in transformers based on linear conversion and density peak clustering (DPC). First, to reduce the complexity of solving the localization equations, the nonlinear localization equations are transformed into linear localization equations by eliminating the second-order terms. Then, to reduce the influence of time delay errors on localization accuracy, the initial localization values are located by multiple acoustic emission (AE) sensors. Finally, the optimal PD coordinates are determined by clustering the initial location values using density peaks clustering algorithm with automatic finding centers (AFC-DPC). The experimental results show that the proposed method can improve PD localization accuracy in transformers, and the average localization error is 5.30 cm.

INDEX TERMS Partial discharge (PD), localization, time difference of arrival (TDOA), acoustic emission (AE) sensors, AFC-DPC.

I. INTRODUCTION

Most power grid failures are caused by insulation defects [1]–[3]. Partial discharge (PD) usually occurs when electrical equipment is defective in insulation [4]. As the primary equipment in the power grid, the insulation status of the transformer directly affects the safe operation of the power grid [5], [6]. The detection of PD is an important method to evaluate the insulation status of transformers [7]. Determining the exact position of the PD source can more accurately reflect the insulation status of the transformer and help the operator to formulate the appropriate maintenance strategies [8]–[10].

The detection of PD localization can usually be divided into the ultra-high-frequency (UHF) method and acoustic emission (AE) method [11]. The UHF method has good anti-interference and high sensitivity, but the installation of UHF sensors still faces some challenges. The transformer tank has an electromagnetic shielding effect, so most UHF sensors must be preinstalled in the transformer. Once the transformer comes into service, it is difficult to install UHF sensors in transformer [12]. Unlike UHF sensor, AE sensor is not affected by external electrical interference and can be easily installed on the enclosure of transformer [13]. Therefore, the AE method has been widely applied in PD localization [14].

When PD occurs, the AE method calculates the time delay in arrival of the acoustic signal. Then the localization equations are established according to the time difference of arrival (TDOA) localization method, and the position of PD is obtained [15]–[17]. This shows that the time delay

The associate editor coordinating the review of this manuscript and approving it for publication was Mehdi Bagheri.

is the crucial parameter in PD localization and solving the localization equations is the key process. However, it is challenging to solve the localization equations characterized by nonlinearity [19]. Besides, due to the interference factors such as the noise of the detection system and the internal structure of the transformer, the time delay data obtained are inevitably errors [18]. These problems will reduce the accuracy of PD localization.

In order to improve localization accuracy, many PD localization algorithms have been reported. The traditional method of solving localization equations is the Newton-Raphson iterative algorithm, but it is prone to local convergence [20], [21]. In addition, the algorithm requires an initial value to be close to the actual position. If the initial value is incorrectly selected, the algorithm cannot converge [12], [19]. To solve the above problems, intelligent optimization algorithms such as particle swarm optimization (PSO) algorithm [14], [22], genetic algorithm (GA) [23], and neural network algorithm [24] have been applied to PD localization. However, these algorithms do not consider the effect of time delay error on PD localization accuracy.

The inner structure of the transformer will cause refraction, reflection and diffraction of the PD signal, thus increasing the time delay error. Some researchers have studied ways to improve the accuracy of time delays. A recent study [25] has established a PD localization model that considers the errors caused by refraction and diffraction. In [26], an improved propagation route search (IPRS) algorithm has been proposed, which can obtain the fastest propagation route of the PD signal. In [4], the acoustic wave propagation inside the transformer has been discussed, and a fiber-optic acoustic sensor array has been designed for PD localization in transformer winding. The article [27] has studied how to locate the PD in the transformer by the macro fiber composite sensors (MFCS). The MFCS can be installed on uneven surfaces and can be applied to transformers of various shapes. However, the time delay detected by the AE sensors will inevitably have errors.

This article proposes a novel PD localization method in transformers based on linear conversion and density peak clustering (DPC). First, eight AE sensors are used to detect PD simultaneously. Then, the nonlinear localization equations are transformed into linear localization equations, and 56 initial localization values are obtained by the Gaussian elimination method. Finally, the optimal coordinates of PD source are determined by clustering the initial location values by using the density peaks clustering algorithm with automatic finding centers (AFC-DPC).

Overall, the main contributions of the article include:

1) Considering the difficulty in solving nonlinear localization equations using existing algorithms, we propose to transform nonlinear localization equations into linear localization equations by eliminating second-order terms.
2) To reduce the impact of time delay errors on localization accuracy and decrease the dependence of algorithm on exact time delay data, PD is simultaneously located by multiple AE sensors. We can obtain multiple initial localization values. Then the optimal coordinates of the PD source are determined by clustering the initial location values.
3) The DPC algorithm needs to determine the cutoff distance manually to calculate the local density, and according to the decision graph manually select the cluster centers. To overcome those two limitations, the proposed AFC-DPC algorithm applies the cutoff distance sequence to calculate the local density. In addition, it uses the γ_i value to determine the cluster centers.

The remainder of this article is organized as follows. In section II, we briefly introduce the principle of PD localization. We proposed a novel localization algorithm based on AFC-DPC in section III. In section IV, simulations and experiments with the localization algorithm are presented. Finally, the conclusions are shown in section V.

II. THEORY OF PD LOCALIZATION IN TRANSFORMERS

A. PRINCIPLE OF TDOA LOCALIZATION

The principle of TDOA localization method is to receive signals from the point to be located through multiple sensors and then obtain the time delay data of the signals reaching each sensor. The nonlinear localization equations are established by using the coordinates and time delay data of each sensor. Finally, the coordinates of the point to be located can be obtained by solving the localization equations.

To determine the PD position in 3D space, at least four or more AE sensors are needed to simultaneously detect the PD signal. Suppose the coordinates of the PD source and AE sensors are P (x, y, z) and S_i (x_i, y_i, z_i) $(i = 1, 2, \ldots, n)$, respectively. According to the principle of TDOA localization, the following localization equations are established:

$$\begin{cases} (x-x_1)^2+(y-y_1)^2+(z-z_1)^2 = v^2t^2 \\ (x-x_2)^2+(y-y_2)^2+(z-z_2)^2 = v^2(t+\tau_{21})^2 \\ (x-x_3)^2+(y-y_3)^2+(z-z_3)^2 = v^2(t+\tau_{31})^2 \\ (x-x_4)^2+(y-y_4)^2+(z-z_4)^2 = v^2(t+\tau_{41})^2 \\ \ldots\ldots \\ (x-x_n)^2+(y-y_n)^2+(z-z_n)^2 = v^2(t+\tau_{n1})^2 \end{cases} \quad (1)$$

where t is the time required for the acoustic wave to reach the first sensor from the PD source. Here, τ_{i1} is the time delay between the acoustic wave from the PD source to reaching the i th $(i = 2, 3, \ldots, n)$ sensor and the first sensor. The velocity of the acoustic wave is v.

The coordinates of the PD source can be obtained by solving the nonlinear localization equations (1).

B. LOCALIZATION MODEL TRANSFORMATION

It is difficult to solve complex nonlinear localization equations. To avoid the above problem, the nonlinear equations are transformed into linear equations by eliminating the second-order terms [28].

Five AE sensors are needed to locate the PD to convert the nonlinear localization equations into linear localization equations. We can get the following equations from (1):

$$(x-x_1)^2+(y-y_1)^2+(z-z_1)^2=v^2t^2 \quad (2)$$
$$(x-x_2)^2+(y-y_2)^2+(z-z_2)^2=v^2(t+\tau_{21})^2 \quad (3)$$
$$(x-x_3)^2+(y-y_3)^2+(z-z_3)^2=v^2(t+\tau_{31})^2 \quad (4)$$
$$(x-x_4)^2+(y-y_4)^2+(z-z_4)^2=v^2(t+\tau_{41})^2 \quad (5)$$
$$(x-x_5)^2+(y-y_5)^2+(z-z_5)^2=v^2(t+\tau_{51})^2 \quad (6)$$

Expand and subtract (2) and (3) to obtain the following equation:

$$(x_2-x_1)x+(y_2-y_1)y+(z_2-z_1)z+v^2\tau_{21}t = 0.5\times\left[\left(x_2^2+y_2^2+z_2^2\right)-\left(x_1^2+y_1^2+z_1^2\right)-v^2\tau_{21}^2\right] \quad (7)$$

Let $x_{i1}=x_i\text{-}x_1, y_{i1}=y_i\text{-}y_1, z_{i1}=z_i\text{-}z_1, l_i=x_i^2+y_i^2+z_i^2$, and $i=2,3,\ldots,5$. Then (7) can be rewritten as follows:

$$x_{21}x+y_{21}y+z_{21}z+v^2\tau_{21}t=0.5\left(l_2-l_1-v^2\tau_{21}^2\right) \quad (8)$$

Similarly, (5), (6), and (7) are expanded and subtracted from (2), respectively, to obtain the following equations:

$$x_{31}x+y_{31}y+z_{31}z+v^2\tau_{31}t=0.5\left(l_3-l_1-v^2\tau_{31}^2\right) \quad (9)$$
$$x_{41}x+y_{41}y+z_{41}z+v^2\tau_{41}t=0.5\left(l_4-l_1-v^2\tau_{41}^2\right) \quad (10)$$
$$x_{51}x+y_{51}y+z_{51}z+v^2\tau_{51}t=0.5\left(l_5-l_1-v^2\tau_{51}^2\right) \quad (11)$$

Equations (8) - (10) can be rewritten into the localization equations as follows:

$$\begin{bmatrix} x_{21} & y_{21} & z_{21} & v^2\tau_{21} \\ x_{31} & y_{31} & z_{31} & v^2\tau_{31} \\ x_{41} & y_{41} & z_{41} & v^2\tau_{41} \\ x_{51} & y_{51} & z_{51} & v^2\tau_{51} \end{bmatrix} \cdot \begin{bmatrix} x \\ y \\ z \\ t \end{bmatrix} = 0.5 \cdot \begin{bmatrix} l_2-l_1-v^2\tau_{21}^2 \\ l_3-l_1-v^2\tau_{31}^2 \\ l_4-l_1-v^2\tau_{41}^2 \\ l_5-l_1-v^2\tau_{51}^2 \end{bmatrix} \quad (12)$$

where $x_{i1}=x_i\text{-}x_1, y_{i1}=y_i\text{-}y_1, z_{i1}=z_i\text{-}z_1, l_i=x_i^2+y_i^2+z_i^2$, and $i=2,3,\ldots,5$.

The Gaussian elimination algorithm can solve the linear localization equations (12), and the coordinates of the PD source can be obtained.

III. MULTI INITIAL LOCALIZATION VALUES CLUSTERING METHOD BASED ON AFC-DPC

A. ACQUISITION OF INITIAL LOCALIZATION VALUES

By using the coordinates and time delay data of a set of AE sensors, an initial localization value can be obtained and expressed as P_1. For PD source at the same position, the coordinates and time delay data of another set of AE sensors are used to substitute into (12). Another initial localization value can also be obtained, expressed as P_2. It can be seen from (12) that the time delay data is the crucial parameter in localization equations. Theoretically, if there is no error in time delays, then P_1 and P_2 are identical. However, due to interference factors such as the noise of the detection system and the internal structure of the transformer, the measured time delays will inevitably produce errors. This will lead to the points P_1 and P_2 being noncoincidence and having some errors with the actual PD position.

To improve the accuracy of PD localization, we use multiple AE sensors to locate PD and obtain multiple initial localization values. Then we can determine the optimal PD coordinates by using a clustering algorithm to reduce the effect of the time delay on the localization accuracy.

Using too many AE sensors will increase detection costs. On the other hand, it will increase the task of solving localization equations and clustering. When too few sensors are utilized, the few initial localization values obtained are not conducive to clustering. Therefore, we use eight AE sensors to detect PD simultaneously in this article. According to (12), any five AE sensors form a group and establish the corresponding localization equations. We can obtain 56 initial localization values by solving these localization equations.

B. AFC-DPC

The DPC algorithm was first proposed by A. Rodriguez and A. Laio. in 2014 [29]. The algorithm is based on the idea that the density of the cluster center is greater than that of the neighbor, and the distance from the point is higher. The algorithm determines the cluster centers by calculating the local densities and distances of the points and then assigns the remaining points to the same clusters with the closest points. As can be seen above, local density and distance are two critical parameters in the DPC algorithm. These two parameters and their calculation methods are described below.

Suppose there is a data set $s=\{x_i\}_{i=1}^N, i=1,2,\ldots,N$. For each data point x_i in the data set s, there is a corresponding local density and distance. Let d_{ij} represents the Euclidean distance between data points x_i and x_j.

$$d_{ij}=\left\|x_i-x_j\right\|_2 \quad (13)$$

There are two calculation methods for the local density ρ_i, (14) and (15) are the cutoff kernel method and the Gaussian kernel method, respectively.

$$\rho_i=\sum_{j=1}^{n}\chi\left(d_{ij}-d_c\right) \quad (14)$$

where $\chi(x)=\begin{cases}1, & x<0\\ 0, & x\geq 0\end{cases}$, and $d_c>0$ is the cutoff distance.

$$\rho_i=\sum_{j=1}^{n}e^{-\left(\frac{d_{ij}}{d_c}\right)^2} \quad (15)$$

The distance δ_i is defined as follows: when the data point x_i has the largest local density, δ_i is the distance of the data point

with the largest distance from x_i in the data set s. Besides, for other data points that do not have the maximum local density, δ_i is the distance from the data point with the smallest distance among all data points with a local density greater than x_i. The formula for calculating δ_i is as follows:

$$\delta_i = \begin{cases} \min\limits_j \left(d_{ij}\right), & \exists j \text{ s.t.} \rho_j > \rho_i \\ \max\limits_j \left(d_{ij}\right), & \text{otherwise} \end{cases} \tag{16}$$

The DPC algorithm is simple and easy to realize. The key to the algorithm is to choose cluster centers based on the local density and distance. Compared with other algorithms, the DPC algorithm only needs to select the cluster centers once, and it does not need to iterate the target function.

However, the DPC algorithm has the following two disadvantages [30]. On the one hand, the cutoff distance d_c is manually selected based on empirical values [31]. The suggestion given in reference [29] is to choose to sort the distance between all data points in ascending order and take the first 1% to 2% as the cutoff distance. For different samples, the clustering results produced by this general cutoff distance selection method may have some errors from the actual results [32], [33]. On the other hand, according to the decision graph, the DPC algorithm manually selects cluster centers with larger ρ_i and δ_i. In order to solve these two problems, an AFC-DPC algorithm is proposed. The AFC-DPC algorithm uses the cutoff distance sequence to calculate the local density to overcome pre-specified cutoff distance. Furthermore, the manual selection of cluster centers based on the decision graph is overcome by determining the cluster center with γ_i value.

1) CUTOFF DISTANCE SEQUENCE AND LOCAL DENSITY

The maximum cutoff distance $d_{\max}$ is defined as

$$d_{\max} = \min_i \left\{ d_i \left| d_i = \max d_{ij}, i, j = 1, 2, \ldots, n \right. \right\} \tag{17}$$

$d_{\max}$ can take all points as its neighbors and is the neighbor radius lower bound containing all points. Therefore, the cutoff distance sequences can be defined as follows:

$$Q = \{ dc_i \left| dc_i = i \times h, h = d_{\max}/n, i = 1, 2, \ldots, n \right. \} \tag{18}$$

The local density of x_i is defined as follows:

$$\rho_i = \sum_{l=1}^{n} \left(\sum_{j=1}^{n} \chi \left(d_{ij} - dc_l \right) / l \right) \tag{19}$$

where $d_{ij} = \left\| x_i - x_j \right\|_2$ and $dc_l \in Q$.

As we can see from (19), the cutoff distance sequence can ensure that the local density of at least one point will be affected by all other points. When Q increases, the difference in the number of points in the neighbor of the same cutoff distance will also be reflected in the local density. Similar to the local density of DPC algorithm with Gaussian kernel, AFC-DPC algorithm also considers the effect of all data points on local density. Every point contributes to the local density. However, their contributions are different, and the farther points have a weaker contribution to the local density [34].

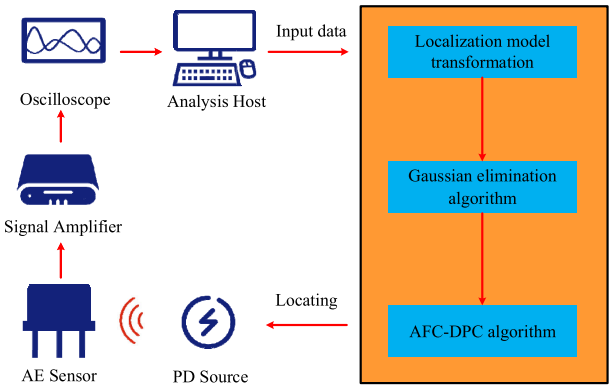

FIGURE 1. Flow chart of proposed PD localization.

2) SELECTION OF CLUSTER CENTERS

For different data sets, the local density and distance of each data point vary. In order to simplify the calculation, the local density ρ_i and distance δ_i are normalized. Then define the γ_i of each data point x_i as follows:

$$\gamma_i = \rho_i \sqrt{\delta_i} \tag{20}$$

where $i = 1, 2, \ldots, n$.

All data points x_i are arranged in descending order according to the magnitude of the γ_i values, and the first u data points are taken as the cluster centers. We take 10% of the number of samples as the number of cluster centers. In other words, we take $u = 6$ in this article.

The DPC algorithm defines the cluster centers with large local density ρ_i and distance δ_i,, and the anomaly points have higher δ_i values and lower ρ_i values. Therefore, in the AFC-DPC algorithm, we have weakened the function of the δ_i value in determining the cluster centers and have defined a quantity γ_i which combines the ρ_i and the δ_i. The larger the γ_i, the more likely they are the cluster centers.

C. AFC-DPC ALGORITHM FLOW

The proposed AFC-DPC algorithm flow is shown in Fig.2 and Table 1.

D. COMPUTATIONAL COMPLEXITY ANALYSIS

Suppose n is the number of data points in the data set, u is the number of clusters, and h is the number of iterations. As shown in Table 2, we choose K-Means, DBSCAN, and DPC to compare the computational complexity with the AFC-DPC algorithm proposed in this article [31], [34].

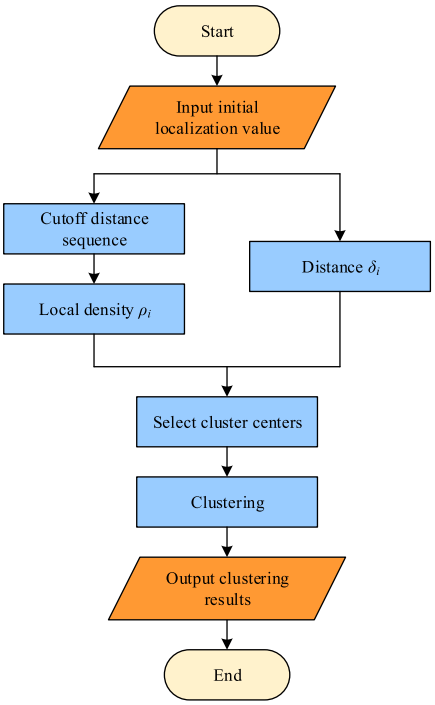

FIGURE 2. Steps for the proposed AFC-DPC algorithm.

TABLE 1. The Proposed AFC-DPC Algorithm Flow.

AFC-DPC algorithm

Input: Data set s

Output: Cluster labels

Calculate the distance matrix using (13).
Find the maximum cutoff distance $d_{\max}$ using (17).
Determine the cutoff distance sequence Q using (18).
for $i = 1$ **to** n **do**
  for $l = 1$ to n **do**
    Calculate the cutoff distance d_{cl}.
  end for
  Calculate local density ρ_i of data point x_i using (19).
end for
for $i = 1$ **to** n in descending order of local density **do**
  Calculate distances δ_i using (16).
end for
for $i = 1$ **to** n **do**
  Calculate γ_i using (20).
end for
Sort γ_i in descending order.
Select cluster number u and cluster centers.
for $i = 1$ **to** n-u in descending order of local density **do**
  Assign remaining point x_i to a cluster with higher local density and the smallest distance.
end for

E. DETERMINATION OF THE OPTIMAL PD SOURCE COORDINATES

After 56 initial localization values are clustered, they will be divided into u clusters. By averaging all the data in each cluster, u points can be obtained, and the coordinates of each point is recorded as $P'_k\left(x'_k, y'_k, z'_k\right)$ $(k = 1, 2, \ldots, u)$.

When the number of AE sensors is eight, the nonlinear localization equations (1) can be written as follows:

$$\begin{cases} \sqrt{(x-x_1)^2+(y-y_1)^2+(z-z_1)^2} = vt \\ \sqrt{(x-x_2)^2+(y-y_2)^2+(z-z_2)^2} = v(t+\tau_{21}) \\ \sqrt{(x-x_3)^2+(y-y_3)^2+(z-z_3)^2} = v(t+\tau_{31}) \\ \vdots \\ \sqrt{(x-x_8)^2+(y-y_8)^2+(z-z_8)^2} = v(t+\tau_{81}) \end{cases} \tag{21}$$

Let $r_i = \sqrt{\left(x'_k - x_i\right)^2 + \left(y'_k - y_i\right)^2 + \left(z'_k - z_i\right)^2}$ subtract the 2nd - 8th equation from the first equation in (21), and the following equations can be obtained:

$$\begin{cases} r_2 - r_1 = v\tau_{21} \\ r_3 - r_1 = v\tau_{31} \\ \vdots \\ r_8 - r_1 = v\tau_{81} \end{cases} \tag{22}$$

Let $\boldsymbol{X}_k = \left(x'_k, y'_k, z'_k\right)^{\mathrm{T}}$, (22) can be rewritten as follows:

$$\boldsymbol{F}\left(\boldsymbol{X}_k\right) = \begin{bmatrix} r_2 - r_1 - v\tau_{21} \\ r_3 - r_1 - v\tau_{31} \\ \vdots \\ r_8 - r_1 - v\tau_{81} \end{bmatrix} = \begin{bmatrix} f_1\left(\boldsymbol{X}_k\right) \\ f_2\left(\boldsymbol{X}_k\right) \\ \vdots \\ f_8\left(\boldsymbol{X}_k\right) \end{bmatrix} \tag{23}$$

If there are no errors in the time delay data, then $\boldsymbol{F}(\boldsymbol{X}_k) = \boldsymbol{0}$. However, there are inevitably errors in the time delay data, so $\boldsymbol{F}(\boldsymbol{X}_k) \neq \boldsymbol{0}$. In other words, $\boldsymbol{F}(\boldsymbol{X}_k)$ can describe the magnitude of the solution error of (22). This article takes the 1 norm of $\boldsymbol{F}(\boldsymbol{X}_k)$ as the evaluation index, and the evaluation index E_k is defined as follows:

$$E_k = \left\|\boldsymbol{F}\left(\boldsymbol{X}_k\right)\right\|_1 \tag{24}$$

Calculate the evaluation index E_k of point P'_k and compare their values. When there are errors in the time delays, the smaller the value of E_k, the smaller the errors of the solution of (21). In other words, the point where the value of the evaluation index is the smallest is closest to the actual PD source. Take this point as the optimal PD source coordinates.

TABLE 2. Computational Complexity Comparisons.

Algorithm	K-Means	DBSCAN	DPC	AFC-DPC
Complexity	$O(hun)$	$O(nlogn)$	$O(n^2)$	$O(n^3)$

F. STEPS OF PD LOCALIZATION METHOD PROPOSED IN THIS PAPER

The main steps of the PD localization method in transformers based on linear conversion and AFC-DPC proposed are shown in Fig. 3.

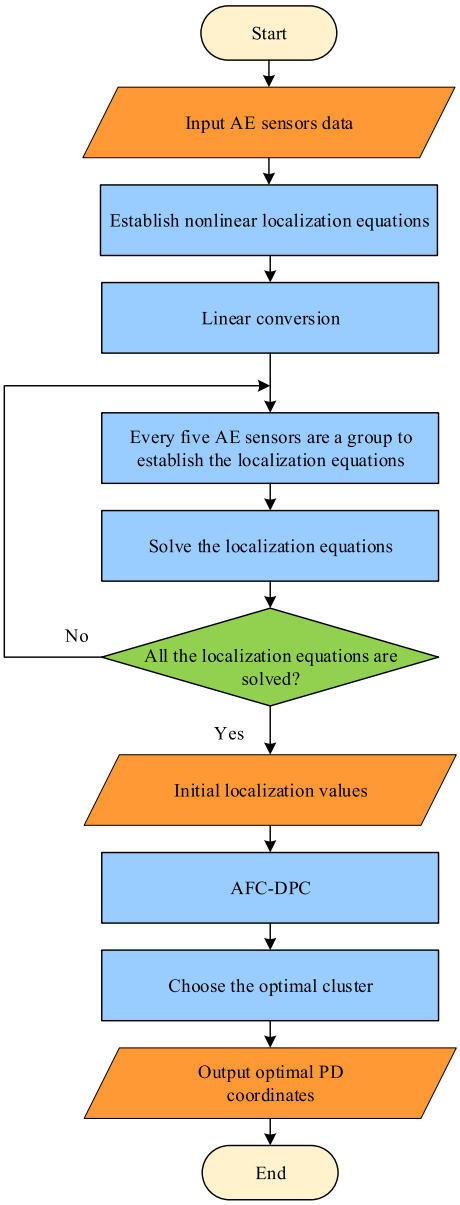

FIGURE 3. Steps of the PD localization method proposed in this article.

IV. SIMULATIONS AND EXPERIMENTS OF THE ALGORITHM

A. NUMERICAL SIMULATIONS

As shown in Fig. 4, the size of the transformer is assumed to be 150cm × 100cm × 120cm. The coordinates of PD source are P (60, 45, 80) cm. The coordinates of the eight AE sensors are S_1 (10, 0, 10) cm, S_2 (10, 100, 10) cm, S_3 (140, 100, 10) cm, S_4 (140, 0, 10) cm, S_5 (20, 0, 110) cm, S_6 (20, 100, 110) cm, S_7 (130, 100, 110) cm, and S_8 (130, 0, 110) cm. The speed of acoustic wave propagating in the oil of transformer is 1500m/s [35].

The theoretical time delays of acoustic waves from the PD source to each sensor can be calculated using the coordinates of each sensor and PD source. In actual detection, there are inevitable errors in the time delays. To verify the correctness

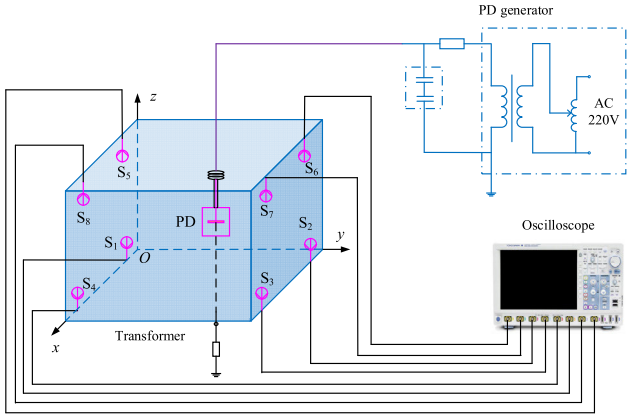

FIGURE 4. Hardware structure of PD localization.

and feasibility of the algorithm, the time delay errors are artificially added based on the theoretical time difference data, which is used to simulate the time delays in actual detection. Suppose that the theoretical time delay is τ, the simulated time delay is τ' after adding the error, and the defined time delay error is e:

$$e = \left| \frac{\tau' - \tau}{\tau} \right| \tag{25}$$

Add five types of random time delays errors within a certain range, which are $e_1 \in (0, 2\%)$, $e_2 \in (2\%, 4\%)$, $e_3 \in (4\%, 6\%)$, $e_4 \in (6\%, 8\%)$ and $e_5 \in (8\%, 10\%)$. The simulated time delay data are shown in Table 3.

TABLE 3. Time Delay Data of Eight AE Sensors.

τ_{i1}	Theoretical time delay (μs)	Simulated time delay (μs)				
		e_1	e_2	e_3	e_4	e_5
τ_{21}	33	34	34	34	35	36
τ_{31}	151	150	146	142	141	136
τ_{41}	122	123	118	129	131	111
τ_{51}	-199	-202	-204	-210	-212	-216
τ_{61}	-152	-150	-158	-144	-141	-140
τ_{71}	-21	-21	-20	-22	-22	-23
τ_{81}	-57	-57	-59	-60	-61	-62

Assuming that the actual coordinates of the PD source are $(x_{act}, y_{act}, z_{act})$ and the coordinates obtained by the localization algorithm are (x, y, z), then the PD localization error is defined as follows

$$\Delta R = \sqrt{(x - x_{act})^2 + (y - y_{act})^2 + (z - z_{act})^2} \tag{26}$$

We define the error on each axis as follows:

$$\Delta x = |x - x_{act}| \tag{27}$$

$$\Delta y = |y - y_{act}| \tag{28}$$

$$\Delta z = |z - z_{act}| \tag{29}$$

Then, the maximum error of coordinates is as follows:

$$D_{max} = \max \{\Delta x, \Delta y, \Delta z\} \tag{30}$$

TABLE 4. Localization Results and Errors Before and After Clustering.

Time delay error	Method	Result (cm)	Error (cm)				
			Δx	Δy	Δz	D_{max}	ΔR
e_1	Before clustering	(60.5,45.1,79.1)	0.5	0.1	0.8	0.9	1.1
	K-means	(60.5,45.1,79.1)	0.5	0.1	0.9	0.9	1.0
	DBSCAN	(61.4,45.4,77.6)	1.4	0.4	2.4	2.4	2.8
	DPC	(60.7,45.2,78.7)	0.7	0.2	1.3	1.3	1.5
	AFC-DPC	**(60.7,45.2,78.7)**	**0.7**	**0.2**	**1.3**	**1.3**	**1.5**
e_2	Before clustering	(62.2,45.7,76.1)	2.2	0.7	1.1	2.2	4.6
	K-means	(62.7,45.8,75.4)	2.7	0.8	4.6	4.6	5.4
	DBSCAN	(58.2,44.4,82.6)	1.8	0.6	2.6	2.6	3.2
	DPC	(60.8,45.2,78.5)	0.8	0.2	1.5	1.5	1.7
	AFC-DPC	**(59.1,44.8,81.3)**	**0.9**	**0.2**	**1.3**	**1.3**	**1.6**
e_3	Before clustering	(62.8,46.0,75.6)	2.8	1.0	4.4	4.4	5.3
	K-means	(58.6,44.9,82.2)	1.4	0.1	2.2	2.2	2.6
	DBSCAN	(58.6,44.9,82.2)	1.4	0.1	2.2	2.2	2.6
	DPC	(62.2,45.5,76.9)	2.2	0.5	3.1	3.1	3.9
	AFC-DPC	**(58.7,44.9,82.1)**	**1.3**	**0.1**	**2.1**	**2.1**	**2.5**
e_4	Before clustering	(45.1,43.0,114.2)	14.9	2	34.2	34.2	37.3
	K-means	(60.6,45.1,79.4)	0.6	0.1	0.6	0.6	0.9
	DBSCAN	(62.4,45.4,76.7)	2.4	0.4	1.7	2.4	4.0
	DPC	(62.2,46.3,76.9)	2.2	1.3	3.1	3.1	4.0
	AFC-DPC	**(60.6,45.1,79.4)**	**0.6**	**0.1**	**0.6**	**0.6**	**0.9**
e_5	Before clustering	(65.7,46.4,71.1)	5.7	1.4	8.9	8.9	10.7
	K-means	(61.9,44.9,77.8)	1.9	0.1	2.2	2.2	2.9
	DBSCAN	(61.9,44.9,77.8)	1.9	0.1	2.2	2.2	2.9
	DPC	(60.0,44.1,81.5)	0	0.9	1.5	1.5	1.7
	AFC-DPC	**(60.0,44.1,81.5)**	**0**	**0.9**	**1.5**	**1.5**	**1.7**

The scatter plots and clustering results of 56 initial localization values under five different time delay errors are shown in Fig. 5. With the increase of time delay errors, the initial localization values are gradually discrete. The 56 initial localization values are clustered by using the AFC-DPC algorithm. A few cluster points are far beyond the scope of the transformer set up by the simulation, so they are not shown. Then, the points in the 6 clusters are averaged, and the optimal PD source coordinates are determined according to the evaluation index E_k.

To compare the localization results and errors before and after clustering, we take an average of 56 initial localization values as the localization results before clustering. At the same time, we compared the localization errors of K-Means, Density-Based Spatial Clustering of Applications with Noise (DBSCAN), DPC, and the proposed AFC-DPC algorithm. The number of clusters in the K-Means algorithm is 6, and the cluster centers are randomly selected. In the DBSCAN algorithm, the radius of the neighborhood is 3, and the core object contains at least 5 samples. The DPC algorithm uses the Gaussian kernel to calculate the local density, chooses to sort the distances between all data points in ascending order and takes the first 2% as the cutoff distance.

The localization results and errors are shown in Fig. 6 and Table 4. We can see that when the time delay error is tiny (for example, the time delay error is e_1), the localization errors before and after clustering are not much different. When the time delay error is e_2, the localization error after using the clustering algorithm is smaller except for the K-Means algorithm. When the time difference error reaches e_3 (that is, the time difference error is greater than 4%), with the time delay error increasing, the localization error after clustering is smaller than before clustering. However, only the AFC-DPC algorithm has the smallest localization errors and highest stability.

The results show that PD localization is very sensitive to the time delay parameter, and the clustering algorithm can effectively reduce the effect of the time delay error. However, compared with other clustering algorithms, only the AFC-DPC algorithm proposed in this article can keep the localization error minimum.

The following takes the data set with time delay error e_5 as an example to analyze the process of the method in this article. First, 56 initial localization values are calculated by Gaussian elimination. The specific data are shown in Table 5. The errors of 56 initial localization values are shown in Fig. 7. There are some errors in time delays, which result in a large dispersion of initial localization values. Besides, the errors of some initial localization values are large, and the PD position cannot be accurately found. The average location result for these 56 initial location values are (65.7,46.4,71.1) cm, and the localization error is 10.7 cm. Then, we use the AFC-DPC algorithm to cluster the 56 initial localization values. According to (19), the local density ρ_i of each data point can be calculated. Then calculate the distance δ_i of each data point according to (16). Finally, the γ_i value of each data point is obtained according to (20). Table 5 shows the local density ρ_i, distance δ_i and γ_i value of each data point. We sort the γi values in descending order and use the first 6 data points as cluster centers. All data in each cluster are averaged, and the evaluation parameter E_k are calculated. As can be seen from Table 6, the evaluation index value corresponding to cluster

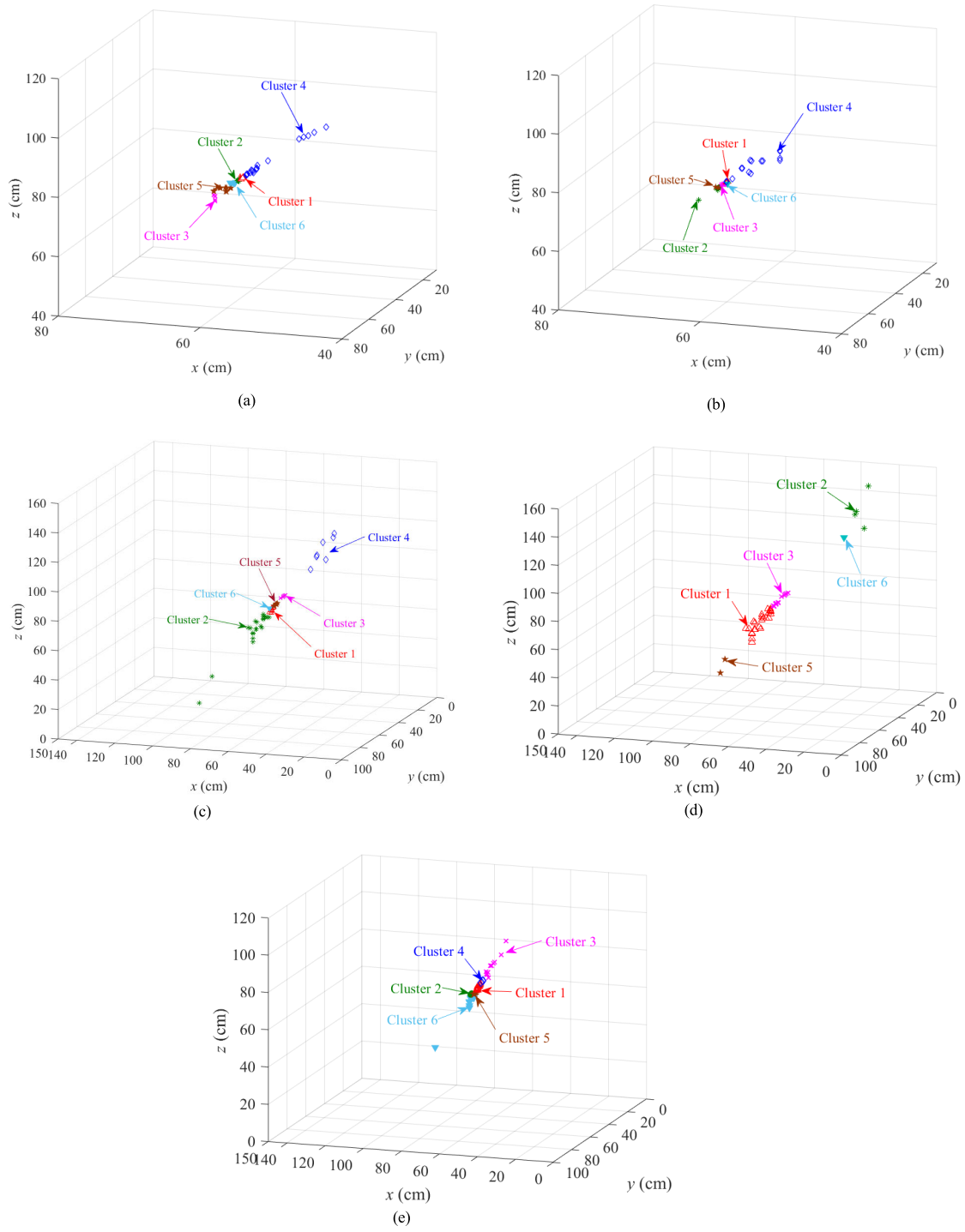

FIGURE 5. The distribution of 56 initial localization clustering results with different time delay errors where (a) time delay error is e_1, (b) time delay error is e_2, (c) time delay error is e_3, (d) time delay error is e_4, and (e) time delay error is e_5.

3 is minimal, which means that the final localization result is (60.0,44.1,81.5) cm and the localization error is 1.7 cm.

B. EXPERIMENTS IN LABORATORY

To verify the effectiveness of the proposed method, we conducted PD localization experiments in the laboratory. As shown in the Fig. 8, the experimental system is composed of a transformer box model, PD generator, AE sensors, and oscilloscope. The size of the transformer tank model is 120cm × 160cm × 105cm. The transformer tank model is made of stainless steel with good electromagnetic shielding performance. The coordinates of the eight AE sensors are S_1 (20, 0, 20) cm, S_2 (20, 160, 20) cm, S_3 (100, 160, 20) cm, S_4 (100, 0, 20) cm, S_5 (30, 0, 80) cm, S_6 (30, 160, 180) cm,

TABLE 5. 56 Initial Localization Values When the Time Delay Error is e_5.

Number	Localization result (cm)			ρ_i	δ_i	γ_i	Cluster label	Number	Localization result (cm)			ρ_i	δ_i	γ_i	Cluster label
	x	y	z						x	y	z				
1	69.7	48.1	60.1	0.277	0.032	0.049	6	29	66.0	46.6	70.4	1.000	1.000	1.000	1
2	69.7	48.1	61.3	0.322	0.049	0.071	6	30	64.1	45.7	74.2	0.519	0.019	0.072	4
3	69.7	48.1	63.4	0.476	0.044	0.100	6	31	61.7	42.1	81.1	0.266	0.062	0.066	3
4	69.7	48.1	63.1	0.454	0.009	0.042	6	32	65.4	45.5	71.2	0.657	0.021	0.095	1
5	67.4	47.0	66.7	0.732	0.022	0.108	5	33	65.4	46.5	71.2	0.839	0.005	0.057	1
6	66.1	46.4	70.4	0.883	0.007	0.073	1	34	61.7	44.8	78.5	0.469	0.018	0.064	3
7	66.4	46.5	69.7	0.801	0.008	0.071	1	35	69.3	47.6	64.9	0.580	0.007	0.048	6
8	64.5	45.6	73.5	0.610	0.003	0.034	4	36	67.9	47.5	65.6	0.642	0.034	0.118	6
9	65.0	45.9	72.5	0.663	0.014	0.080	1	37	66.6	47.1	69.5	0.757	0.014	0.091	1
10	60.2	43.6	82.0	0.271	0.108	0.089	3	38	66.4	47.0	70.2	0.902	0.008	0.079	1
11	67.1	47.0	66.8	0.712	0.006	0.053	5	39	64.5	46.4	73.5	0.608	0.014	0.073	4
12	65.1	46.1	72.0	0.727	0.022	0.108	1	40	62.2	45.6	79.2	0.365	0.033	0.066	3
13	65.4	46.3	71.2	0.843	0.020	0.119	1	41	67.6	47.4	67.4	0.756	0.027	0.125	5
14	61.7	44.7	78.6	0.467	0.002	0.020	3	42	64.5	44.2	73.5	0.479	0.040	0.096	4
15	62.0	44.8	77.8	0.499	0.118	0.171	3	43	66.4	46.0	69.2	0.671	0.019	0.094	1
16	59.2	43.6	83.3	0.253	0.044	0.053	3	44	66.4	46.7	69.9	0.925	0.015	0.112	1
17	68.5	47.0	66.6	0.779	0.024	0.121	6	45	64.5	45.8	73.5	0.680	0.045	0.145	4
18	68.2	47.0	66.7	0.767	0.006	0.057	6	46	83.1	57.4	41.0	0.000	0.704	0.000	6
19	55.2	43.6	88.1	0.121	0.147	0.046	3	47	61.8	43.5	75.3	0.364	0.077	0.101	3
20	58.6	43.6	84.0	0.227	0.025	0.036	3	48	65.9	46.6	70.7	0.873	0.009	0.084	1
21	67.7	47.5	65.3	0.628	0.007	0.053	6	49	62.0	44.9	77.9	0.493	0.003	0.025	3
22	65.8	46.9	70.2	0.859	0.008	0.078	1	50	69.3	47.6	65.2	0.605	0.039	0.119	6
23	65.4	46.8	71.2	0.837	0.008	0.073	1	51	69.2	47.5	67.1	0.893	0.000	0.006	2
24	61.7	45.7	77.6	0.413	0.025	0.066	3	52	69.1	47.5	67.0	0.896	0.113	0.301	2
25	52.8	43.1	95.6	0.043	0.221	0.020	3	53	68.7	47.4	67.5	0.758	0.002	0.036	2
26	67.4	47.4	67.4	0.715	0.005	0.049	5	54	68.8	47.4	67.5	0.845	0.014	0.099	2
27	66.5	45.6	70.7	0.657	0.025	0.104	1	55	69.3	47.6	66.9	0.831	0.004	0.055	2
28	67.0	46.3	68.7	0.632	0.022	0.094	1	56	69.3	47.6	66.9	0.829	0.000	0.000	2

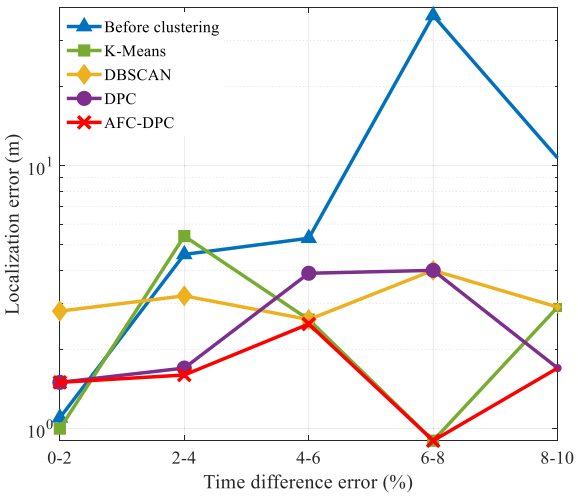

FIGURE 6. Localization errors before and after clustering.

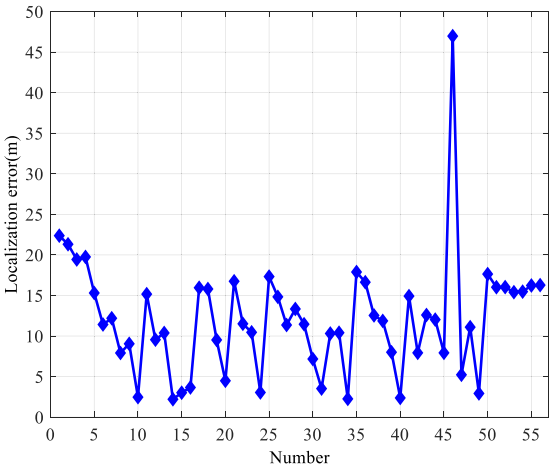

FIGURE 7. The localization errors of 56 initial localization values when time delay error is e_5.

TABLE 6. Clustering Results When the Time Delay Error is e_5.

Cluster	Localization result (cm)	Localization error (cm)	E_k
1	(65.9,46.4,70.5)	11.3	37.83
2	(69.1,47.5,67.2)	15.9	52.71
3	(60.4,44.1,81.5)	1.7	9.13
4	(64.4,45.5,73.7)	7.8	24.34
5	(67.4,47.2,67.1)	15.1	52.31
6	(70.2,48.5,62.1)	20.9	73.74

S_7 (90, 160, 80) cm, and S_8 (90, 0, 80) cm, respectively. The diameter of the AE sensor is 25mm, the center frequency is 40kHz, and the receiving sensitivity is greater than -68dB. The PD sources are set at PD_1 (80, 60, 40) cm and PD_2 (50, 120, 50) cm, respectively. The PD generating device is composed of a boosting transformer and a protrusion defect model. The oscilloscope sampling rate is set at 250ks/s. The inside of the transformer tank model is not filled with oil, so the speed of acoustic wave in the air is 340 m/s. The time-domain waveforms of PD signals are shown in Figure 9, and the time delay data are shown in Table 7.

We use the localization method proposed in this article to locate two PD sources. The clustering distribution of the initial localization values obtained is shown in Fig. 10. Some points outside the transformer range are not plotted in Fig. 10. The clustering results are shown in Table 8 and Table 9.

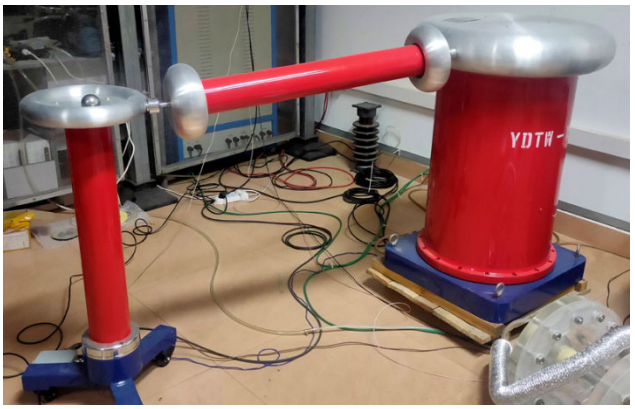

(a)

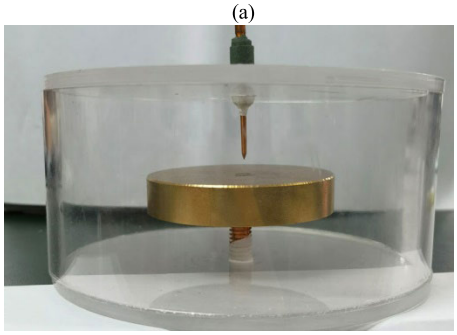

(b)

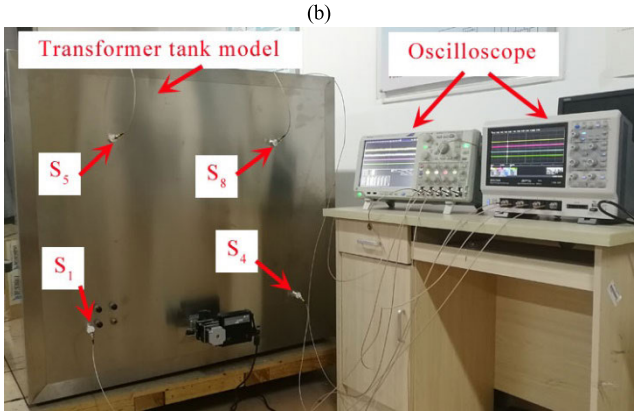

(C)

FIGURE 8. PD localization experiments in a laboratory where (a) is a boosting transformer, (b) is a protrusion defect model, and (c) is the PD localization system.

TABLE 7. Time Delay Data of Eight Sensors for PD $_1$ and PD $_2$.

τ_{i1}	PD_1 (μs)	PD_2 (μs)
τ_{21}	965	-2144
τ_{31}	461	-1578
τ_{41}	-648	168
τ_{51}	18	-60
τ_{61}	880	-2051
τ_{71}	661	-1930
τ_{81}	-445	84

According to the evaluation parameter E_k, the optimal PD source coordinates are finally determined. As shown in Table 10, the localization errors of PD_1 and PD_2 are 2.4cm and 8.2cm, respectively. The average localization error of the two PD sources is 5.3cm.

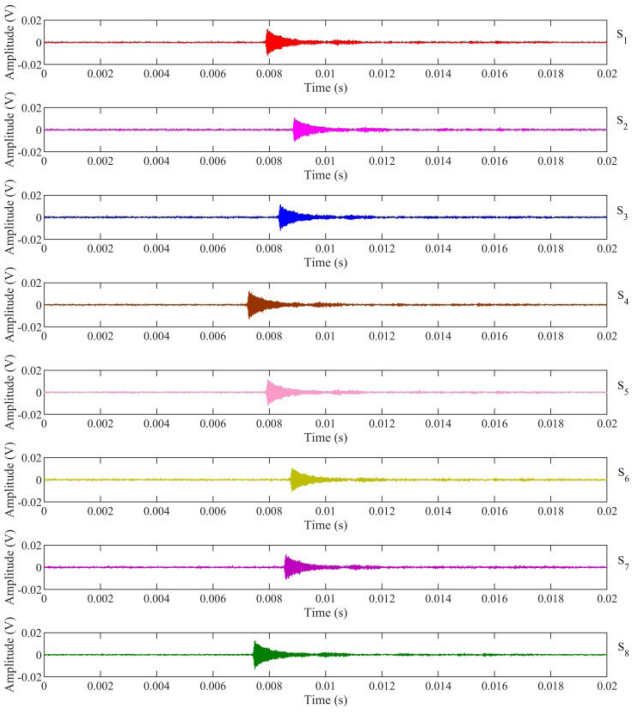

(a)

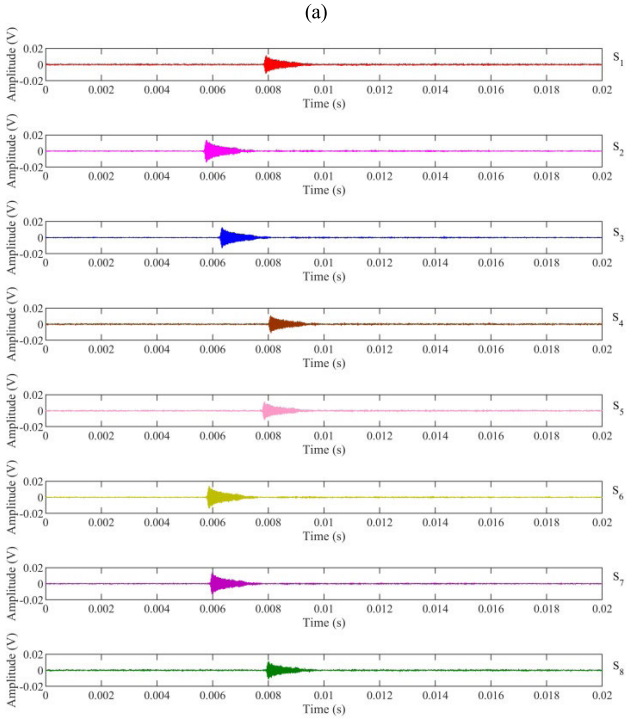

(b)

FIGURE 9. The time-domain waveforms of the PD signals where (a) is PD_1 signal and (b) is PD_2 signal.

To compare the localization results and errors before and after clustering, we take an average of 56 initial localization values as the localization results before clustering. Table 10 shows that the localization errors after clustering using the AFC-DPC algorithm are smaller than before.

In [12], methods such as the Newton-Raphson algorithm, Chan algorithm, genetic algorithm (GA), and imperialist

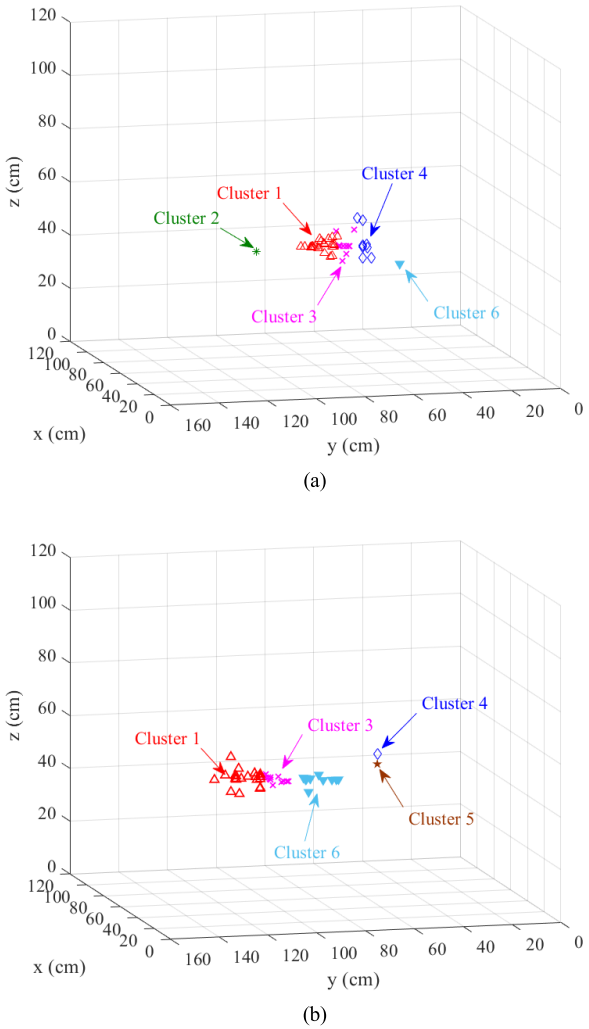

FIGURE 10. The distribution of 56 initial localization clustering results where (a) is the results of PD_1 and (b) is the results of PD_2.

TABLE 8. Clustering Results for PD_1.

Cluster	Localization result (cm)	Localization error (cm)	E_k
1	(63.0,76.3,44.1)	23.9	113.68
2	(-4.4,133.8,57.2)	113.4	445.72
3	(78.3,61.6,40.6)	2.4	13.21
4	(95.4,47.9,37.8)	19.7	70.96
5	(-115.6,249.8,34.3)	272.6	568.48
6	(514.6,-406.8,-116.7)	656.8	328.92

TABLE 9. Clustering Results for PD_2.

Cluster	Localization result (cm)	Localization error (cm)	E_k
1	(51.7,112.1,48.4)	8.2	51.47
2	(135.6,-368.8,-16.9)	500.7	908.28
3	(57.0,92.2,46.6)	23.1	186.06
4	(93.4,43.1,46.3)	88.4	509.28
5	(66.7,52.3,48.4)	69.7	457.66
6	(59.3,79.8,45.0)	41.6	272.96

competitive algorithm (ICA) are used for PD localization in transformer. We take average errors as the errors of these methods. The comparison results are shown in Table 11.

TABLE 10. Localization Results and Errors Before and After Clustering for PD_1 and PD_2.

PD source		PD_1	PD_2
Before clustering	Localization result (cm)	(106,8,30.1,28.1)	(67.6,30.7,37.9)
	Localization error (cm)	41.9	72.5
After clustering	Localization result (cm)	(78.3,61.6,40.6)	(51.7,112.1,48.4)
	Localization error (cm)	**2.4**	**8.2**

TABLE 11. Error Analysis and Comparison of Localization Results of Various Methods.

Method	Error (cm)				
	Δx	Δy	Δz	$D_{\max}$	ΔR
Newton-Raphson	5.67	6.00	1.33	6.00	12.23
Chan	14.00	7.33	1.00	14.00	16.93
GA	13.00	7.00	3.00	13.00	14.90
ICA	2.33	10.00	8.67	10.00	15.20
Proposed method	1.70	4.75	1.05	4.75	5.30

As can be seen from Table 11, the errors of the method proposed in this article are smaller than other methods. The results show that the proposed method can accurately locate PD in transformers.

V. CONCLUSION AND FUTURE WORKS

This article proposes a novel PD localization method in transformers based on linear conversion and AFC-DPC. The nonlinear localization equations are transformed into linear localization equations. Multiple initial localization values are obtained by simultaneous detection of PD by multiple AE sensors. The AFC-DPC algorithm is used to perform cluster optimization on multiple initial localization values to determine the optimal coordinates of the PD source.

1) To reduce the difficulty of solving the localization equations, we transform the nonlinear localization equations into linear localization equations by eliminating the second-order terms.
2) To decrease the influence of the time delay errors on the localization accuracy, the initial localization values are clustered by using the AFC-DPC algorithm.
3) The AFC-DPC algorithm uses the cutoff distance sequence to calculate the local density and uses the γ_i to determine the clustering centers, which overcomes the limitations of the DPC algorithm and improves the clustering performance of the algorithm.

The effectiveness and accuracy of the method are verified by simulation and experiments. Simulation results show that when the time delay error is 8%-10%, the localization error is 1.7cm. The experiment results show that the average localization error is 5.3cm. Compared with the errors of other

localization methods, the method proposed in this article has the advantages of the low localization error.

In future work, we will undertake the following two studies:

1) We will study methods for extracting precise time delays. The influence of the inner structure of the transformer on the refraction and diffraction of the PD signal can be reduced.
2) To improve the precision of PD localization in transformers, we will further study the new localization algorithm.

REFERENCES

[1] M. Wu, H. Cao, J. Cao, H.-L. Nguyen, J. B. Gomes, and S. P. Krishnaswamy, "An overview of state-of-the-art partial discharge analysis techniques for condition monitoring," *IEEE Elect. Insul. Mag.*, vol. 31, no. 6, pp. 22–35, Nov. 2015.

[2] W. J. K. Raymond, H. A. Illias, A. H. A. Bakar, and H. Mokhlis, "Partial discharge classifications: Review of recent progress," *Measurement*, vol. 68, pp. 164–181, May 2015.

[3] N. A. Al-geelani, M. A. M. Piah, and N. Bashir, "A review on hybrid wavelet regrouping particle swarm optimization neural networks for characterization of partial discharge acoustic signals," *Renew. Sustain. Energy Rev.*, vol. 45, pp. 20–35, May 2015.

[4] C. Gao, L. Yu, Y. Xu, W. Wang, S. Wang, and P. Wang, "Partial discharge localization inside transformer windings via fiber-optic acoustic sensor array," *IEEE Trans. Power Del.*, vol. 34, no. 4, pp. 1251–1260, Aug. 2019.

[5] A. Akbari, P. Werle, H. Borsi, and E. Gockenbach, "Transfer function-based partial discharge localization in power transformers: A feasibility study," *IEEE Elect. Insul. Mag.*, vol. 18, no. 5, pp. 22–32, Sep. 2002.

[6] C. Pan, J. Tang, Y. Zhang, X. Luo, and X. Li, "Variation of discharge characteristics with temperature in moving transformer oil contaminated by metallic particles," *IEEE Access*, vol. 6, pp. 40050–40058, 2018.

[7] L. Luo, B. Han, J. Chen, G. Sheng, and X. Jiang, "Partial discharge detection and recognition in random matrix theory paradigm," *IEEE Access*, vol. 5, pp. 8205–8213, 2017.

[8] A. U. M. Zaki, Y. Hu, and X. Jiang, "Partial discharge localization in 3-D with a multi-DNN model based on a virtual measurement method," *IEEE Access*, vol. 8, pp. 87434–87445, 2020.

[9] Z. Guozhi, X. Zhang, H. Xingrong, Y. Jia, J. Tang, Z. Yue, T. Yuan, and L. Zhenze, "On-line monitoring of partial discharge of less-oil immersed electric equipment based on pressure and UHF," *IEEE Access*, vol. 7, pp. 11178–11186, 2019.

[10] M. Homaei, S. M. Moosavian, and H. A. Illias, "Partial discharge localization in power transformers using neuro-fuzzy technique," *IEEE Trans. Power Del.*, vol. 29, no. 5, pp. 2066–2076, Oct. 2014.

[11] C. Gao, W. Wang, S. Song, S. Wang, L. Yu, and Y. Wang, "Localization of partial discharge in transformer oil using Fabry-Pérot optical fiber sensor array," *IEEE Trans. Dielectr. Electr. Insul.*, vol. 25, no. 6, pp. 2279–2286, Dec. 2018.

[12] Y.-B. Wang, D.-G. Chang, Y.-H. Fan, G.-J. Zhang, J.-Y. Zhan, X.-J. Shao, and W.-L. He, "Acoustic localization of partial discharge sources in power transformers using a particle-swarm-optimization-route-searching algorithm," *IEEE Trans. Dielectr. Electr. Insul.*, vol. 24, no. 6, pp. 3647–3656, Dec. 2017.

[13] W. M. F. Al-Masri, M. F. Abdel-Hafez, and A. H. El-Hag, "A novel bias detection technique for partial discharge localization in oil insulation system," *IEEE Trans. Instrum. Meas.*, vol. 65, no. 2, pp. 448–457, Feb. 2016.

[14] R. A. Hooshmand, M. Parastegari, and M. Yazdanpanah, "Simultaneous location of two partial discharge sources in power transformers based on acoustic emission using the modified binary partial swarm optimisation algorithm," *IET Sci., Meas. Technol.*, vol. 7, no. 2, pp. 112–118, Mar. 2013.

[15] H. Hou, G. Sheng, and X. Jiang, "Robust time delay estimation method for locating UHF signals of partial discharge in substation," *IEEE Trans. Power Del.*, vol. 28, no. 3, pp. 1960–1968, Jul. 2013.

[16] F. Zeng, J. Tang, L. Huang, and W. Wang, "A semi-definite relaxation approach for partial discharge source location in transformers," *IEEE Trans. Dielectr. Electr. Insul.*, vol. 22, no. 2, pp. 1097–1103, Apr. 2015.

[17] H. H. Sinaga, B. T. Phung, and T. R. Blackburn, "Partial discharge localization in transformers using UHF detection method," *IEEE Trans. Dielectr. Electr. Insul.*, vol. 19, no. 6, pp. 1891–1900, Dec. 2012.

[18] W. M. F. Al-Masri, M. F. Abdel-Hafez, and A. H. El-Hag, "Toward high-accuracy estimation of partial discharge location," *IEEE Trans. Instrum. Meas.*, vol. 65, no. 9, pp. 2145–2153, Sep. 2016.

[19] M.-X. Zhu, Y.-B. Wang, D.-G. Chang, G.-J. Zhang, X. Tong, and L. Ruan, "Quantitative comparison of partial discharge localization algorithms using time difference of arrival measurement in substation," *Int. J. Electr. Power Energy Syst.*, vol. 104, pp. 10–20, Jan. 2019.

[20] P. J. Moore, I. E. Portugues, and I. A. Glover, "Radiometric location of partial discharge sources on energized high-voltage plant," *IEEE Trans. Power Del.*, vol. 20, no. 3, pp. 2264–2272, Jul. 2005.

[21] Q. Zhang, C. Li, S. Zheng, H. Yin, Y. Kan, and J. Xiong, "Remote detecting and locating partial discharge in bushings by using wideband RF antenna array," *IEEE Trans. Dielectr. Electr. Insul.*, vol. 23, no. 6, pp. 3575–3583, Dec. 2016.

[22] L. Tang, R. Luo, M. Deng, and J. Su, "Study of partial discharge localization using ultrasonics in power transformer based on particle swarm optimization," *IEEE Trans. Dielectr. Electr. Insul.*, vol. 15, no. 2, pp. 492–495, Apr. 2008.

[23] Z. Tang, C. Li, X. Cheng, W. Wang, J. Li, and J. Li, "Partial discharge location in power transformers using wideband RF detection," *IEEE Trans. Dielectr. Electr. Insul.*, vol. 13, no. 6, pp. 1193–1199, Dec. 2006.

[24] T. Boczar, S. Borucki, A. Cichon, and D. Zmarzly, "Application possibilities of artificial neural networks for recognizing partial discharges measured by the acoustic emission method," *IEEE Trans. Dielectr. Electr. Insul.*, vol. 16, no. 1, pp. 214–223, Feb. 2009.

[25] J. Jia, C. Hu, Q. Yang, Y. Lu, B. Wang, and H. Zhao, "Localization of partial discharge in electrical transformer considering multi-media refraction and diffraction," *IEEE Trans. Ind. Informat.*, early access, Sep. 14, 2020, doi: 10.1109/TII.2020.3023883.

[26] Y.-B. Wang, Y.-H. Fan, S.-R. Qin, D.-G. Chang, X.-J. Shao, H.-B. Mu, and G.-J. Zhang, "Partial discharge localisation methodology for power transformers based on improved acoustic propagation route search algorithm," *IET Sci., Meas. Technol.*, vol. 12, no. 8, pp. 1023–1030, Nov. 2018.

[27] B. A. de Castro, D. de Melo Brunini, F. G. Baptista, A. L. Andreoli, and J. A. C. Ulson, "Assessment of macro fiber composite sensors for measurement of acoustic partial discharge signals in power transformers," *IEEE Sensors J.*, vol. 17, no. 18, pp. 6090–6099, Sep. 2017.

[28] S. Wang, Y. He, B. Yin, S. Ning, and W. Zeng, "Partial discharge localization in substations using a regularization method," *IEEE Trans. Power Del.*, early access, May 14, 2020, doi: 10.1109/TPWRD.2020.2994660.

[29] A. Rodriguez and A. Laio, "Clustering by fast search and find of density peaks," *Science*, vol. 344, no. 6191, pp. 1492–1496, Jun. 2014.

[30] D. Yu, G. Liu, M. Guo, X. Liu, and S. Yao, "Density peaks clustering based on weighted local density sequence and nearest neighbor assignment," *IEEE Access*, vol. 7, pp. 34301–34317, 2019.

[31] M. D. Parmar, W. Pang, D. Hao, J. Jiang, W. Liupu, L. Wang, and Y. Zhou, "FREDPC: A feasible residual error-based density peak clustering algorithm with the fragment merging strategy," *IEEE Access*, vol. 7, pp. 89789–89804, 2019.

[32] L. Sun, R. Liu, J. Xu, and S. Zhang, "An adaptive density peaks clustering method with Fisher linear discriminant," *IEEE Access*, vol. 7, pp. 72936–72955, 2019.

[33] M. Parmar, D. Wang, X. Zhang, A.-H. Tan, C. Miao, J. Jiang, and Y. Zhou, "REDPC: A residual error-based density peak clustering algorithm," *Neurocomputing*, vol. 348, pp. 82–96, Jul. 2019.

[34] M. Guo, D. Yu, G. Liu, X. Liu, and S. Cheng, "Drug-target interaction data cluster analysis based on improving the density peaks clustering algorithm," *Intell. Data Anal.*, vol. 23, no. 6, pp. 1335–1353, Nov. 2019.

[35] Q. Xie, Y. Li, F. C. Lü, C. Li, N. Wang, and Y. J. Ding, "Method for PD location in oil combining ultrasonic phased array with wideband array signal processing," *Proc. Chin. Soc. Elect. Eng.*, vol. 29, no. 28, pp. 15–19, 2009.

SHUDONG WANG (Graduate Student Member, IEEE) was born in Anhui, China, in November 1992. He received the B.S. degree in automation from Anhui Polytechnic University, Wuhu, China, in 2015. He is currently pursuing the Ph.D. degree in electrical engineering with the Hefei University of Technology, Hefei, China.

His current research interests include partial discharge detection and localization technology for power equipment.

YIGANG HE (Member, IEEE) was born in Hunan, China. He received the M.S. degree in electrical engineering from Hunan University, Changsha, China, in 1992, and the Ph.D. degree in electrical engineering from Xi'an Jiaotong University, Xi'an, China, in 1996.

In 1990, he joined the College of Electrical and Information Engineering, Hunan University, and was promoted as an Associate Professor and a Professor in 1996 and 1999, respectively. He was a Senior Visiting Scholar with the University of Hertfordshire, Hatfield, U.K., in 2002. From 2006 to 2011, he was the Director of the Institute of Testing Technology for Circuits and Systems, Hunan University. From 2011 to 2017, he was also the Head of the School of Electrical Engineering and Automation, Hefei University of Technology, Hefei, China. In December 2017, he joined Wuhan University, Wuhan, China, where he is currently the Vice Head of the School of Electrical Engineering and Automation. His current research interests include testing and fault diagnosis of analog and mixed-signal circuits, electrical signal detection, smart grid, and intelligent signal processing. He was the Winner of the National Science Fund for Distinguished Young Scholars and National Excellent Science and Technology Worker.

BAIQIANG YIN was born in Hunan, China. He received the B.S. degree in electrical engineering from Nanhua University, Hengyang, China, in 2008, and the Ph.D. degree in electrical engineering from Hunan University, Changsha, China, in 2014.

In 2014, he joined the Hefei University of Technology, Hefei, China, where he is currently an Associate Professor of the School of Electrical Engineering and Automation. His research interests include testing and fault diagnosis of analog and mixed-signal circuits, electrical signal detection, radio frequency identification technology, and intelligent signal processing.

WENBO ZENG was born in Hunan, China, in August 1994. He received the B.S. degree from Hunan University, Changsha, China, in 2016. He is currently pursuing the Ph.D. degree in electrical engineering with the Hefei University of Technology, Hefei, China.

His current research interests include wireless communication channel modeling, key technologies for wireless sensor, and wireless communication testing in smart grids.

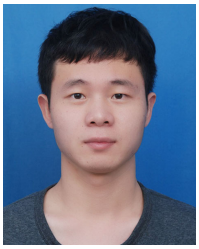

YING DENG was born in Anhui, China, in 1996. He received the B.S. degree in automation from the Anhui University of Science and Technology, Huainan, China, in 2018. He is currently pursuing the M.S. degree with the electrical engineering with the Hefei University of Technology, Hefei, China.

His research interests include digital signal processing and deep learning.

ZENGCHAO HU was born in Anhui, China, in 1995. He received the B.S. degree in electrical engineering and automation from the Anhui University of Science and Technology, Anhui, China, in 2018. He is currently pursuing the M.S. degree in electrical engineering with the Hefei University of Technology, Anhui.

His research interests include power quality disturbance analysis and signal processing.